Book of Tutorials and Abstracts

European Microbeam Analysis Society

EMAS 2026

15th

REGIONAL WORKSHOP

TOPICAL CONFERENCE ON ELECTRON BACKSCATTER DIFFRACTION (EBSD)

14 to 17 June 2026
at the
CentraleSupélec, Gif-sur-Yvette, France

Organised in collaboration with:
ICMMO, ENS Paris-Saclay,
Université Paris-Saclay

EMAS
European Microbeam Analysis Society eV
www.microbeamanalysis.eu/

This volume is published by:
European Microbeam Analysis Society eV (EMAS)
EMAS Secretariat
c/o Eidgenössische Technische Hochschule, Department of Earth and Planetary Sciences
Clausiusstrasse 25
8092 Zürich
Switzerland

ISBN 978 90 8227 6992
NUR code: 971 – Materials Science

ELECTRON CHANNELLING CONTRAST IMAGING (ECCI):
A SEM-based technique for crystal defect imaging in bulk materials

Nathalie Gey* and N. Maloufi

CNRS Université de Lorraine Arts et Métiers Institute of Technology, LEM3, Metz, France
e-mail: nathalie.gey@univ-lorraine.fr

Nathalie Gey is a Senior Researcher at CNRS, conducting her research at the LEM3 Laboratory (University of Lorraine – CNRS UMR 7239 – Arts et Métiers ParisTech). As a metallurgist specialising in orientation-based SEM microscopy, she has pioneered advanced configurations for data acquisition, including static 3D-EBSD, accurate-ECCI, and direct electron detection, as well as advanced post-processing methods for orientation data, such as crystallographic parent map reconstruction, phase transformation-induced texture modelling, and AI-assisted orientation map analysis. Her work focusses on analysing phase transformation-induced microtextures in steels and titanium alloys to elucidate the process–microstructure–anisotropy relationships in mechanical properties. She has co-authored over 100 peer-reviewed papers and supervised 17 PhD students.
Key roles and responsibilities: Deputy director of LEM3 (since January 2024) | Work package leader for the Labex DAMAS (2012–2024) | Co-chair of the International Conference on Textures of Materials (ICOTOM 2024, Metz) | Course leader for “CNAM Entreprise” training programme "Pratique de l’EBSD".

1. INTRODUCTION

Electron channelling contrast imaging (ECCI) is a scanning electron microscopy (SEM) based technique that enables high resolution imaging and analysis of crystallographic extended defects (e.g., dislocations, twins, stacking faults) underneath the surface of bulk materials. Transmission electron microscopy (TEM) is the reference technique for studying crystalline defects [1]. However, it requires thinned samples, thereby limiting observations to very small regions of interest. Moreover, the thin foil preparation process can often alter the defect structure under investigation. While SEM is highly versatile for surface imaging using secondary electron (SE) and backscattered electron (BSE) detectors, conventional SEM imaging lacks the contrast mechanisms necessary to directly visualize defects in bulk materials.

ECCI bridges the gap between TEM and SEM by providing non-destructive, high-resolution imaging of defects in a wide range of materials, including semiconductors (GaN, SiC), ceramics ($SrTiO_3$, UO_2), and metals such as advanced steels (TWIP, interstitial-free-steel). Its ability to operate in a standard SEM, to explore different areas of a bulk sample paving the way for more representative studies, and without the need for sample thinning makes it an accessible and powerful tool for researchers in both academia and industry.

The foundations of ECCI were laid in the 1960s, with the observation of Kikuchi-like pattern by Coates [2] and a qualitative interpretation of the phenomenon by Booker [3], who suggested using the strong variation in backscattered electrons (BSE) yield as a function of the angle between the incident electron beam and the crystal planes to contrast crystal defects. This phenomenon, known as electron channelling, forms the basis of ECCI contrast: When the beam is close to the Bragg condition of a given low-index crystallographic planes, the BSE yield changes sharply, producing orientation-dependent contrast and thus visualisation or contrast for example of sub-grain boundaries and dislocations. However, early applications of ECCI were limited by two major challenges: (1) The poor spatial resolution of electron channelling patterns (ECP) limited to single crystals, which were used to determine orientation and set channelling conditions, and (2) The limited imaging performance of the SEMs available at the time.

Over the last decade, ECCI has experienced an increase of interest and use for imaging dislocation structures and stacking faults in the near-surface region of bulk materials, thin films, and various substrates [4-8]. This can be attributed to two key developments:

- Advancement in SEM technology with high-performance field-emission gun scanning electron microscopes (FEG-SEMs) has significantly improved the resolution and sensitivity of ECCI. Modern FEG-SEMs offer higher brightness, smaller probe sizes, and better signal-to-noise ratios, enabling high-resolution defect imaging that was previously unattainable.
- Development of new methodologies and tools for setting channelling conditions, such as electron backscatter diffraction (EBSD) assisted orientation mapping and high-resolution selected area channelling patterns (HR-SACP) has improved the accuracy and precision of

ECCI [9-12]. These methods allow researchers to precisely set channelling conditions, even in polycrystalline materials, expanding ECCI's applicability to a wide range of engineering materials.

This tutorial paper reviews the fundamental principles of ECCI, including its experimental setup. It details practical methodologies and tools for accurately setting channelling conditions, such as using ECP, SACP, and EBSD-assisted approaches. Advanced applications such as resolving dislocations in GaN, interstitial-free (IF) steel, and uranium oxide are highlighted, alongside case studies from the authors' research teams [4, 13, 14]. Finally, challenges, limitations, and future directions are highlighted, with the overall aim of guiding researchers in implementing ECCI for materials characterisation.

2. *PRINCIPLE OF ELECTRON CHANNELLING IN SEM*

In a SEM, a focussed electron beam scans the sample surface. Electrons, typically accelerated under voltages up to 30 kV, interact with the material through elastic and inelastic scattering, producing various types of re-emissions [15]. Among these, BSE corresponds to incident electrons deflected by atomic nuclei. The BSE yield is highly sensitive to the material's atomic number Z (the higher the Z, the greater the BSE intensity), and also to the crystal's orientation relative to the incident beam, as illustrated by Fig. 1.

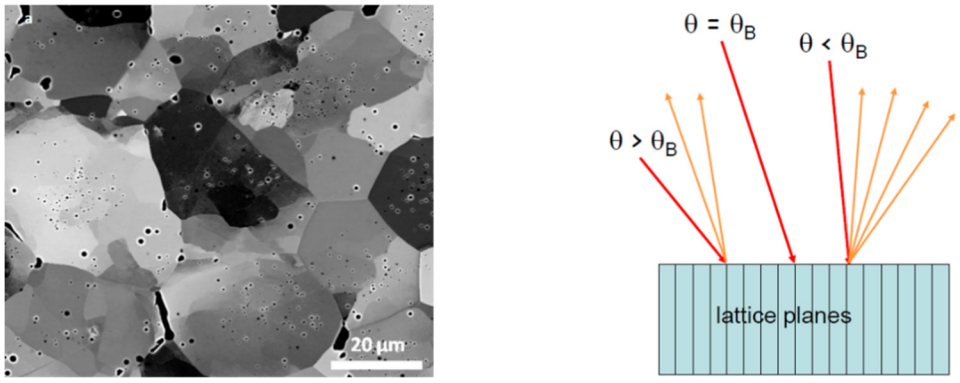

a) b)

Figure 1. a) BSE image revealing grain orientation contrast in an UO_2 sample deformed by creep; b) Change in BSE yield with the angle θ between the crystal lattice planes and the incident electron beam.

ECCI leverages this dependence of the BSE yield on the specimen's orientation relative to the beam. When the electron beam scans a single-crystal, the incidence angle (θ) of the primary beam with respect to different planes varies sufficiently to reach the Bragg diffraction conditions ($\theta = \theta_B$) for

specific {*hkl*} planes. The Bragg angle (θ_B) is the angle for which constructive interference occurs, defined by: $n\lambda = 2d \sin(\theta_B)$, where n is an integer (n = 1 for first-order diffraction), λ the electron wavelength, and d the {*hkl*} plane spacing.

As highlighted Fig. 2a, near the Bragg condition for available (*hkl*) lattice planes, the BSE yield changes abruptly and reaches a minimum at a specific angle $\theta = \theta c$. This intensity minimum is interpreted in terms of electron channelling. It occurs for a slightly positive angular deviation relative to the Bragg angle θ_B ($\Delta\theta_B = \theta - \theta_B > 0$): The electrons are channelled along the atomic rows or planes, reducing backscattering probability and producing a black BSE image in Fig. 2c.

Conversely, when the beam does not satisfy this condition the electrons penetrating the crystal undergo more scattering events, increasing the BSE yield. For $\Delta\theta_B < 0$, the BSE yield increases sharply producing a white appearance or light colour in the BSE image (Figs. 2a and 2b).

Finally, ECCI contrasts defects because distortions in the lattice (e.g., near a dislocation) disrupt channelling, locally increasing the BSE signal. Consequently, channelling conditions are no longer satisfied locally around the defect, and the BSE yield varies strongly, contrasting the defect (Fig. 2d).

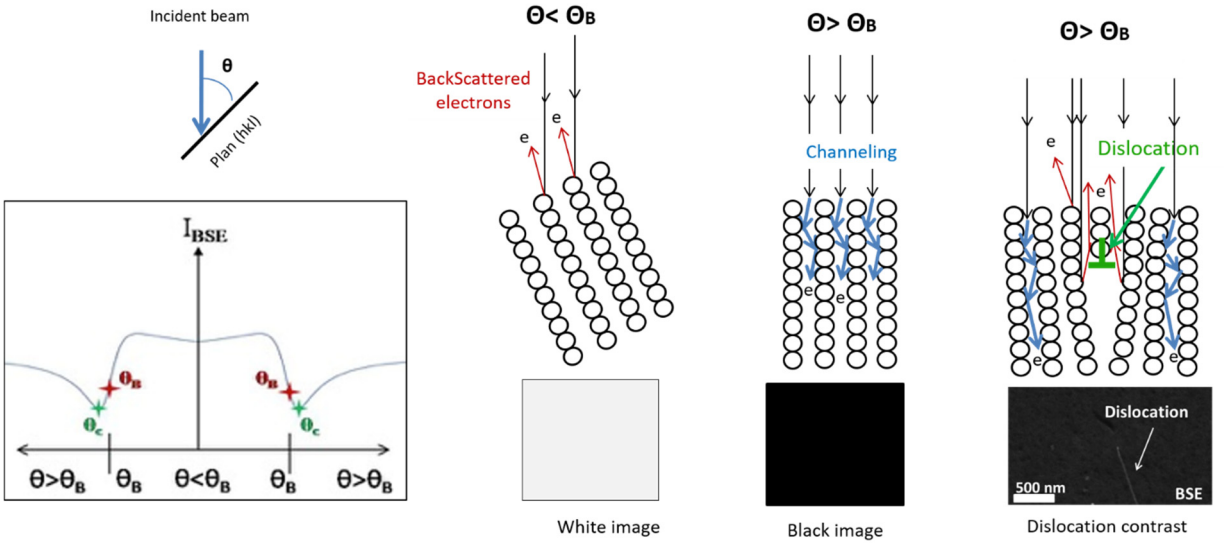

Figure 2. a) BSE intensity variation for a (*hkl*) band in the two-wave approximation as a function of the incidence angle θ between the primary beam and the lattice planes; b) Significant BSE yield for $\Delta\theta_B < 0$, producing white appearance in the BSE image; c) BSE yield is minimised when channelling occurs (perfect crystal) producing black contrast in the BSE image; and d) Increases again near defects due to local lattice distortion producing a sharply intensity change in the BSE image.

The dynamic theory of electron diffraction provides a powerful framework for understanding ECCI contrast. It describes the incident electrons in a crystal as Bloch waves that undergo multiple scattering events coupling the excited waves and redistribute their intensity making a rigorous many-beam treatment necessary for quantitative predictions [15-19]. The relative excitation of each Bloch wave is determined by the orientation of the incident beam with respect to the crystal lattice, through the boundary conditions applied at the crystal surface. For thin specimen regions necessary for TEM studies or near-surface channelling conditions relevant to ECCI, the two-beam approximation, valid when the beam is oriented close to the Bragg condition for a single set of lattice planes, is often used to simplify calculations [15, 20, 21]. Under this two-beam condition ($g = 0$ and $g = (hkl)$), where g is the diffraction vector, it was suggested that two types of Bloch waves are strongly excited and thus predominate, and all others may be neglected reducing the many-beam problem to a tractable two-beam case. This two-beam approximation is easier to handle mathematically and adequately accounts for the intensity contrasts of defects observed in ECCI. In particular, for an incidence angle θ slightly greater than the Bragg angle θ_B, the electron probability density is localised between the (*hkl*) atomic planes, leading to weak scattering and strongly enhanced propagation in the crystal [15, 20]. This results in the electron channelling phenomenon in the crystal, also known as anomalous absorption.

While for θ lower than θ_B the second type wave has its probability density maxima centred directly on the atomic columns promoting intense interactions that result in efficient backscattering and rapid attenuation of the wave as it propagates into the crystal. At Bragg condition the two type waves are excited. It is precisely this difference in absorption between the two Bloch waves that underlies the channelling contrast exploited in ECCI. In fact, when an extended defect is present, its associated strain field locally distorts the atomic planes on its vicinity and alters the balance of excitation between the two Bloch waves and modifies the local BSE yield producing a localised bright or dark feature in the ECC image (Fig. 2) [15, 20].

The purpose of this chapter is not to provide a detailed presentation of the theories and approximations used so far to understand the complex physical processes due to the strong electron-matter interaction. For further details about physical and mathematical aspects to simulate the channelling contrast, see dedicated papers [15, 18, 22, 23].

However, the result of such simulations allows to better exploit the high-potential of ECCI for microstructural characterisation. In particular, these different studies have highlighted the link of different physical parameters on the ECCI contrast such as:

- The Burgers vector (**b**) of the dislocation,
- The diffraction vector (**g**).

The dislocation contrast presents an intensity oscillation (black-white or dark-light) with a periodicity of $\xi\mathbf{g}$ (the extinction distance) depending on the beam energy for the active diffraction vector **g**: $\xi\mathbf{g} = \pi mvVc/\ h\ F(\theta_B)$ (m and v are mass and velocity of the electron

respectively, h Plank constant, Vc cell volume, F the crystal structure factor) [14]. In particular, the visibility depth (also called penetration of electrons) of a dislocation in ECCI is approximately 5ξg [18, 20]. For example, for steel: $\xi_{01\text{-}1}$ = 14.2 nm at an accelerating voltage of 20 kV [14], that means a visibility depth of ~ 71 nm. Table 1 gives some values of ξg (in nm) for three diffraction conditions at 20 kV.

Table 1. ξg (in nm) for different diffraction conditions at 20 kV.

g	111	220	311
ξg Al	25	50	95
ξg Si	26	33	60
ξg Cu	13	14	25

3. *EXPERIMENTAL SETUP AND REQUIREMENT FOR HIGH CONTRAST ECCI*

The experimental setup to acquire ECCI images is schemed Fig. 3. The bulk sample with a well-prepared surface is rotated and tilted to reach a controlled channelling condition in a high-resolution FEG SEM and the ECC signal is acquired on the BSE detector. Two sample tilt configurations have been experienced: Low-tilt with the sample nearly horizontal (up to 30° tilt), and High-tilt with the sample tilted between 55 ~ 70° (similar to EBSD).

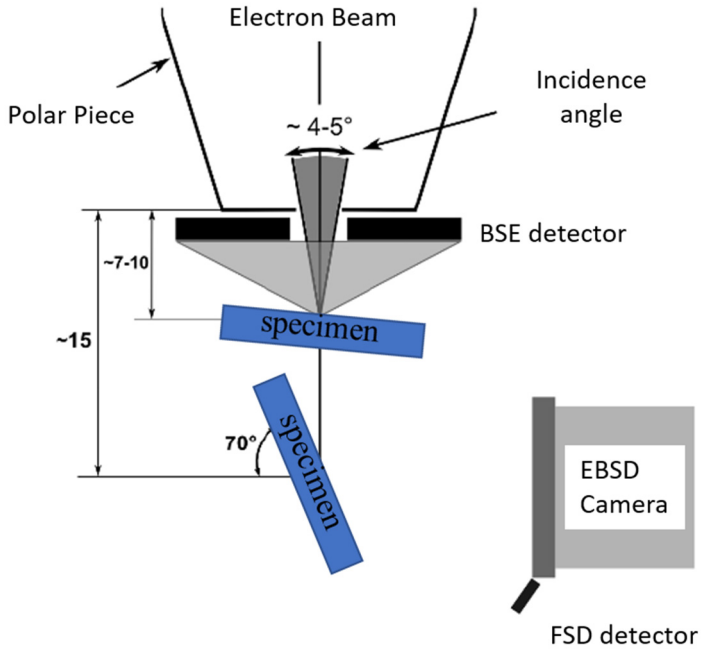

Figure 3. SEM setup for ECC Imaging: In low-tilt, the sample is facing the BSE detector where as in high-tilt or high inclination, the sample is facing the EBSD camera, and the signal is collected on the FSD detector.

This section describes the specific requirements related to the instrument, the BSE detector and the sample surface preparation for high contrast ECC imaging. Remember that a key point to set accurately the channelling condition for ECCI is the need to control the crystal orientation relative to the incident electron beam in the range of 0.1°. This point is detailed in the next section and is especially critical to apply the well-known transmission electron microscopy **g.b** = 0 and **g.bxu** = 0 invisibility criteria [10, 24].

3.1. Sample preparation

ECCI is surface-sensitive: The BSE signal originates from a depth of ~10 to ~100 nm (depending on material and beam energy). Dislocations are visible only if they are within ~5ξg of the surface (typically ~50 to ~100 nm for metals at 20 keV).

Thus, the protocol for the surface preparation is similar as for EBSD analysis. Mechanical polishing is performed using abrasive papers of decreasing grit size, lubricated with water, followed by final polishing steps with diamond paste. Depending on the material, mechanochemical, electrolytic polishing with a suitable solution, or ion polishing can be applied to remove the damaged surface layer and achieve a mirror finish. The key is to avoid introducing defects during surface preparation (for further details, see the tutorial contribution of Grzegorz Cios in this book).

Thin films can be observed directly since they are typically prepared under strict cleanliness conditions and have very low roughness compared to bulk materials.

Additionally, the sample must be conductive or semiconductive to avoid charging effects. Although it is now possible to obtain high-quality SEM images of insulating materials at very low voltages (< 5 kV) or using variable pressure SEM. ECCI images and channelling patterns are currently acquired at voltages above 10 kV. However, with improved detectors and the availability of high-resolution analytical FEG-SEMs at low and high voltages and variable pressure, the range of possibilities is expanding.

3.2. SEM requirements

Intensity calculations based on the dynamic of electron diffraction theory models have defined criteria for achieving optimal ECCI contrast [25, 26 for a summary of related papers]. Among them the different electron beam characteristics are of major importance:

(1) A high probe current (in a nA range) is required to improve the signal-to-noise ratio for good intensity contrast,
(2) A fine probe size is needed to improve lateral spatial resolution to distinguish the defect (~ 5 to10 nm in modern FEG-SEMs). The in-depth resolution is limited by the invisibility distance (~10 to 100 nm).
(3) Low beam divergence (a few mrad) to maintain coherent diffraction conditions.

The dislocation contrast is maximal at a depth from the material surface of 0.2ξg, the probe diameter should be less than (g·b)ξg /5 [27] or (g·b)ξg /4 [18], and the beam divergence should be less than 1/(|g|ξg), where ξg is the extinction distance.

The typical accelerating voltage is between 15 to 30 kV to balance between spatial resolution and beam penetration. Finally, a specimen tilt/rotation stage is required for setting the channelling conditions orientation control. Rocking beam option with improved spatial resolution is also an advantage, as discussed in the next section [11, 12].

In general, most of the required conditions are met in many modern FEG-SEMs.

3.3. Detectors according to the tilt configuration

ECC images are acquired at high magnification (e.g., 10,000×) on a BSE detector.

3.3.1. For low-tilt ECCI. The sample is nearly horizontal (0 < tilt < 30°) and the BSE detector below the pole piece is used (solid-state diodes, YAG detector). Promising results have recently been published on a pixelated detector [28-29]. Working distance has to be adapted to the SEM configuration chamber with the BSE detector inserted, in general short (7 - 10 mm) to maximise BSE collection while maintaining the tilt possibilities. Energy filtering (optional) can improve contrast by removing lower-energy electrons. This low tilt configuration minimizes topographic effects while optimising orientation effects (ideal for defect analysis).

3.3.2. For high-tilt ECCI. The sample is tilted up to ~70° (similar to EBSD) and the forward scatter diodes (FSD) attached to the EBSD camera are used to collect the signal. Optimised camera insertion and WD allows optimal FSD signal collection. This high-tilt configuration is less flexible to set precisely different diffraction conditions. It has been widely applied for features characterisation in semiconductors such as atomic steps and threading dislocations in GaN for example.

4. METHODOLOGIES FOR SETTING CHANNELLING CONDITIONS IN ECCI

To perform ECCI characterisation, even if the probe and BSE detector are suitable, it is also necessary to satisfy channelling conditions for specific (*hkl*) planes of the crystal. This means the crystal must be oriented with high precision (≤ 0.1°) relative to the incident electron beam.

This section reviews the different methodologies available for setting these channelling conditions, such as using ECP, SACP, and EBSD-assisted orientation approaches with high-resolution SACP (HR-SACP). Different software packages are also available to assist users in predicting the specimen stage tilts and rotations necessary to bring a crystal into optimum channelling conditions for ECCI: Astro-ECP [30], TOCA [9], ATEX [31].

4.1. Acquisition of electron channelling patterns (ECP)

On a single-crystal or coarse-grained polycrystalline sample (with millimetre-sized grains), the easiest way to determine the crystal orientation relative to the incident electron beam is the acquisition of an ECP. This involves collecting the BSE signal at very low magnification. As illustrated in Fig. 4a, when the primary beam scans the sample surface, different (*hkl*) planes will successively meet the Bragg incidence and channelling conditions, resulting in a modulated BSE yield that forms a channelling pattern. An example of an ECP pattern collected on a silicon (100) single crystal at 0° tilt is given in Fig. 4a.

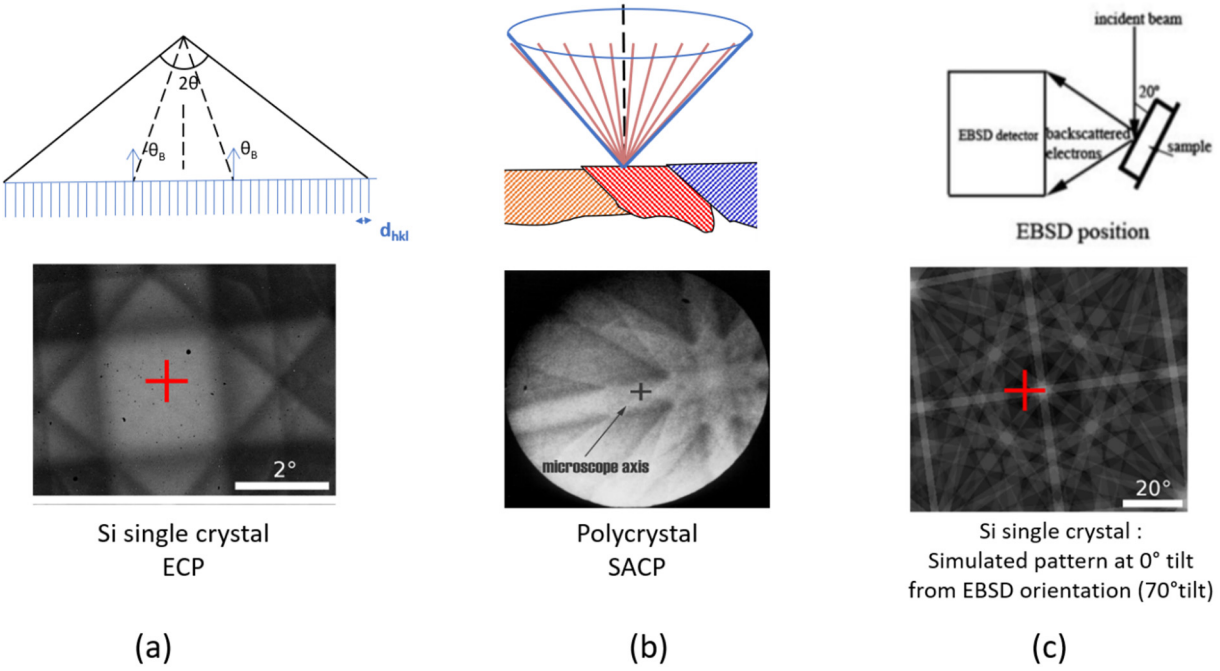

Figure 4. Different approaches to set the channelling conditions, a) ECP acquisition - example on a Si single crystal; b) SACP acquired on a polycrystal; c) Simulation of the pattern at 0° tilt from orientation determined by EBSD at 70° tilt - example on the same Si crystal in a) (the cross indicates the pattern centre).

The pattern centre (PC) i.e., trace of the undeflected incident electron beam on the Kikuchi pattern gives the orientation of the crystal relative to the incident beam. To satisfy a given diffraction condition for a set of (*hkl*) planes the crystal must be oriented (tilt and rotation) until this PC coincides with the edge of a Kikuchi (*hkl*) band.

Since an ECP pattern has a high opening angle (depending on the SEM beam shift amplitude), the patterns can be easily indexed, and successive tilts of the crystal effectively explore the diffraction sphere (or Kikuchi sphere). These Kikuchi patterns are highly sensitive to crystal orientation and can detect very small orientation variations (~0.1°).

Despite its excellent angular resolution of 0.1°, this technique suffers from a spatial resolution on the order of a millimetre, making it unsuitable for characterising fine-grained polycrystalline materials.

4.2. Acquisition of selected area channelling patterns (SACP)

For polycrystalline materials, the previous approach requires that the channelling pattern be collected from an area that lies within the grain of interest. This has historically been achieved by collecting a SACP. The electron beam is precessed around the microscope axis, with the pivot point of the precession cone coinciding with the sample surface so that only a limited area of the sample contributes to the BSE signal. This capability is commonly referred to as "rocking-beam" (see Fig. 4b [24]) . While it was available on older microscopes, it disappeared from many electron columns over the years. However, due to the renewed interest in ECCI, this option has been reimplemented by some manufacturers. In general, the pattern is collected from an area that can reach 20 µm in diameter, with an opening angle up to 20° to facilitate indexing of the different (*hkl*) planes.

The limited spatial resolution of SACPs is a limitation for ECCI applications in fine-grained materials. Additionally, quantitative analysis of dislocations using ECCI is also difficult, as the SACP ideally needs to be collected over the smallest possible area. Any significant rotations across the grain, most commonly from geometrically necessary dislocations, will distort the pattern, making it difficult to identify the optimum channelling bands.

4.3. Acquisition of EBSD patterns at 70° tilt

EBSD offers an alternative approach for collecting diffraction information with much higher spatial resolution than SACP (on the order of a few tens of nanometres, depending on operating conditions and the material) and a high relative angular resolution of about 0.5° (depending on the operation conditions).

However, EBSD determines orientations on highly tilted crystals (typically 70°), and the resulting absolute orientation accuracy in the microscope reference frame is limited to 1 - 2°. Consequently, applying EBSD to set up specific channelling conditions is not straightforward, as ECCI requires the crystal orientation to be controlled relative to the electron beam trajectory (optic axis) within 0.1°.

Comparing ECP acquired at 0° tilt and simulated from the orientation determined by EBSD at 70° tilt (as seen in Figs. 4a and 4c on a Si single crystal) illustrates the uncertainty in beam position introduced by the accuracy limitations of EBSD and the uncertainty of SEM stage control, making it impossible to reliably reach the target channelling conditions [11].

Gutierrez-Urrutia *et al.* [9] have used EBSD orientation analysis to predict the specimen stage tilts and rotations necessary to bring a crystal into optimum channelling conditions for ECCI at low tilts, a procedure known as controlled electron channelling contrast imaging (cECCI). Unfortunately, without direct control of the final sample position in the SEM at low inclination, it is difficult to confirm whether the channelling conditions have been met with the precision required for quantitative ECCI analysis. Thus, it is often necessary to adjust the orientation manually to achieve optimum contrast, and the exact deviation from the Bragg condition cannot be assessed. Nevertheless, using this method, interesting results comparing theoretical images or profiles of backscattered intensity from defects (dislocations, stacking faults, etc.) with experimental ECCI images or profiles have been published [21].

4.4. Series of rotation-ECCI

Lafond *et al.* [32] developed an original approach, called eCHORD (electron channelling orientation determination), for orientation mapping in an SEM equipped with a BSE detector. The method is based on the analysis of the contrast variation of grains due to the channelling of incident electrons on a rotating sample. At each pixel of the map, experimental intensity profiles as a function of the rotation angle are obtained and compared with simulated ones to retrieve the orientation. The relative angular resolution is estimated to be better than 1°.

Based on this concept, the rotation-ECCI (R-ECCI) method involves the automated recording of a series of images during an user-defined rotation of the sample. For each pixel of the region of interest (ROI), the variation of intensity as a function of the rotation angle is obtained and called an intensity profile. The series of images are automatically analysed to determine the dislocation density using these intensity profiles. The R-ECCI method, coupled with clustering algorithm, enables the characterisation of dislocation densities in a material, particularly in deformed materials with local disorientation [33].

4.5. HR-SACP assisted by EBSD

By combining HR-SACP with EBSD-assisted orientation simulations, a procedure called Accurate-ECCI (A-ECCI) offers an attractive solution for setting channelling conditions, providing both high spatial resolution and high angular resolution relative to the incident beam [10, 11].

The developments of a rocking beam mode in the Gemini column have demonstrated HR-SACP patterns with a high spatial resolution, allowing the study of defects in grains as small as 0.5 µm in diameter. For precise crystal orientation determination and band indexing, since the angular range of the HR-SACP pattern is limited to ~4°, the HR-SACP pattern is superimposed on the Kikuchi pattern at 0° simulated from the orientation determined by EBSD (70° tilt).

For some materials, the channelling patterns are so complex that only a dynamic simulation, revealing the intensity modulations of the bands, allows the HR-SACP and EBSD patterns to coincide. The centre of the HR-SACP pattern, corresponding to the microscope axis, then provides the absolute crystal orientation with a precision better than 0.1°, which is optimal for establishing channelling conditions for fine ECCI or A-ECCI analysis.

5. ADVANCED APPLICATIONS EXAMPLES

5.1. Dislocation arrangement into low-angle sub-boundaries in UO_2

This section illustrates the potential of A-ECCI imaging for visualising dislocations and their arrangement into low-angle sub-boundaries induced during the creep of UO_2 at 1,500 °C. These sub-boundaries were previously identified in EBSD orientation maps. The network of sub-boundaries formed in a sintered UO_2 pellet after dislocation creep was examined in detail in [34, 35].

HR-SACPs were collected using a Zeiss Auriga 40 FEG-SEM equipped with a GEMINI-type electron column. All images were acquired at a working distance of 7 mm, an accelerating voltage of 20 kV, and a beam current of 550 pA (with the 30 µm centre aperture). The rocking beam mode was calibrated to achieve sub-micrometre-resolution SACPs, as demonstrated in [11]. This resolution enables the acquisition of HR-SACPs over UO_2 sub-grains.

Figure 5 provides an example of an HR-SACP acquired from the UO_2 sample at zero tilt. The HR-SACP was manually indexed using the Kikuchi pattern simulated from the approximate orientation deduced by EBSD. To achieve the desired two-beam channelling conditions and image the dislocations in the grain of interest, the sample was then rotated and tilted using the precise information extracted from the HR-SACP. Finally, at the expected channelling position, a last HR-SACP was acquired to confirm the sample orientation relative to the incident beam before A-ECCI analysis.

EBSD was used to reveal very low-angle boundaries, down to 0.1°, as seen in Fig. 6. This angular resolution was achieved by optimising EBSD data collection and processing with improved Hough transform option available in Aztec (Oxford Instruments), referred to as "refine accuracy mode". Subsequently, A-ECCI successfully imaged the dislocations produced by creep directly in the bulk sample. The dislocations were mostly organised into sub-boundaries with low-energy configurations, while only a limited number of isolated dislocations were observed.

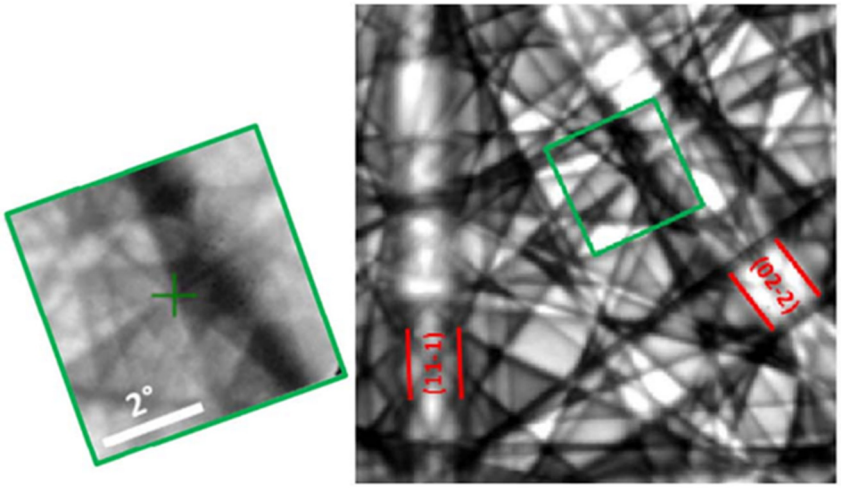

Figure 5. a) HR-SACP collected from UO_2; b) The corresponding dynamically simulated pattern. The green cross in the HR-SACP indicates the microscope optical axis [34].

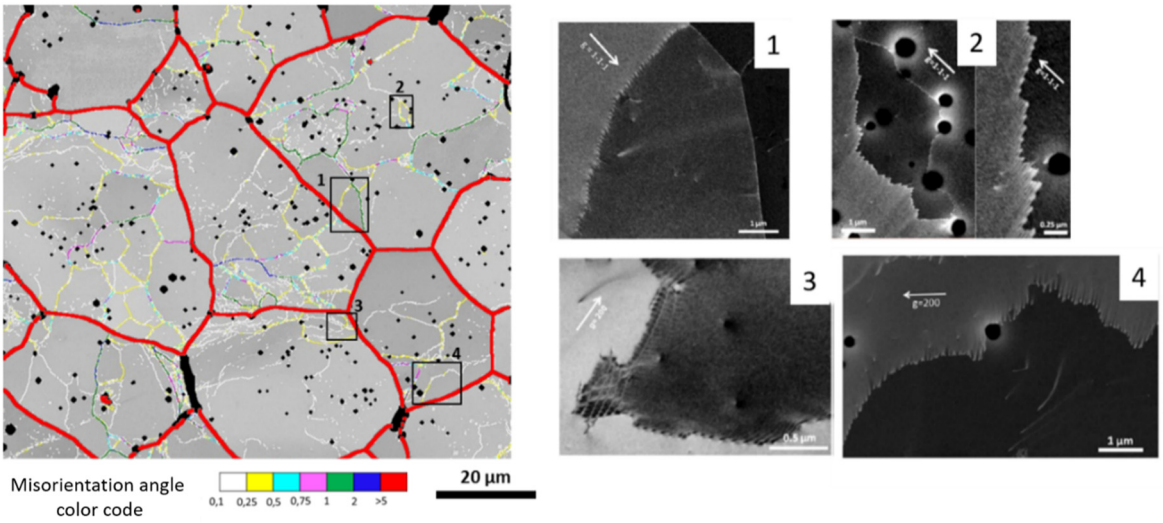

Figure 6. A-ECCI micrographs (numbered 1 to 4) showing different types of dislocation arrangements in low-angle sub-boundaries identified on the EBSD map. Sample: UO_2 deformed by 8 % via dislocation creep at 1,500 °C [34].

5.2. Analysis of threading dislocations in GaN

Gallium nitride (GaN) is one of the most strategically important semiconductor materials due to its exceptional physical properties such as a wide direct bandgap of 3.4 eV, high electron mobility, outstanding thermal stability, and high breakdown electric field that make it suited for high-frequency, high-power electronic devices as well as solid-state lighting applications [36, 37]. In parallel, GaN light-emitting diodes (LEDs) and laser diodes have revolutionised the solid-state lighting industry [38].

However, this material faces a persistent crystallographic problem: the high density of threading dislocations (TDs) that arise during epitaxial growth, primarily due to the large lattice mismatch and thermal expansion coefficient difference between GaN and its most common substrates, sapphire and silicon [39]. Typical TDs densities in heteroepitaxial GaN films range from 10^8 to 10^{10} cm^{-2}, orders of magnitude higher than in common semiconductor systems such as silicon or GaAs. These extended defects act as non-radiative recombination centres, current leakage pathways, and scattering sites for charge carriers, directly degrading device efficiency, reliability, and lifetime [34, 40]. Accurate assessment of TD density and character more generally in nitride (AlN, GaN, AlGaN, ...) based semiconductors structures is indispensable for optimising epitaxial growth strategies, including epitaxial lateral overgrowth (ELO) and substrate engineering, as well as for predicting and improving device performance.

In this section we describe how ECCI is a non-destructive characterisation technique with improved spatial resolution [6, 7, 14, 41, 42] suited for semiconductors. Figure 7 presents an ECC micrograph recorded at an accelerating voltage of 20 keV in the forescatter geometry (high tilt) of a 3.5 µm GaN thin film deposited on c-plane sapphire substrate by metalorganic vapour phase epitaxy (MOVPE).

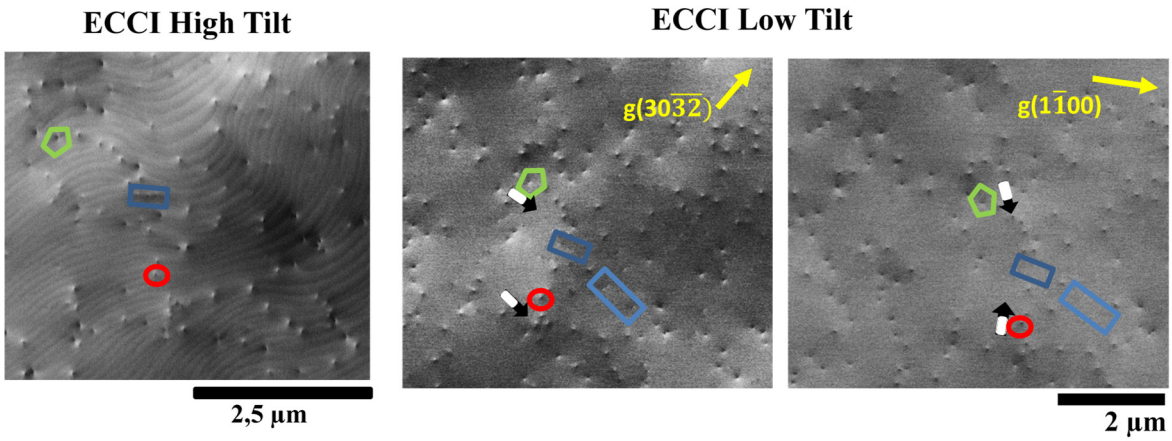

Figure 7. ECC micrographs at high and low tilt of the same zone of a thin GaN film deposited on sapphire substrate. The arrows indicate dark-light contrast direction which rotates with g rotation as illustrated by the two diffraction conditions at low tilt. Blue rectangle, red circle, and green pentagon highlight edge, screw and mixed dislocations respectively (From [14]).

The small misorientations between neighbouring sub-grains produce subtle grey level variations visible in this micrograph. Atomic steps are also visible. Threading dislocations appear as spots with dark-light contrast most of them along sub-grain boundaries, individual dislocations are also present. Due to surface relaxation, the invisibility criteria cannot be applied to threading screw and mixed dislocations in GaN.

However, by recording ECC micrograph under several diffraction conditions and systematically comparing the resulting contrast, it becomes possible to distinguish between the three types of dislocations: Edge (**b** = 1/3⟨11-20⟩), screw (**b** = ⟨0001⟩), and mixed (**b** = 1/3⟨11-23⟩) and to determine their relative densities.

In the low-tilt ECCI micrographs acquired from the same area under two diffraction conditions, under the (30-3-2) condition, which reveals all dislocation types, screw dislocations outlined in red are identified by a black-white contrast that remains consistently perpendicular to the diffraction vector **g**. While mixed dislocations, outlined by green pentagons, display a contrast that varies with changes in **g**. Furthermore, the invisibility criterion **g**.**b** = 0 is applicable for edge dislocations (outlined here by blue rectangles) under which they are rendered out of contrast for the (1-100) condition. For more details for dislocation analysis see [6, 14, 41, 42].

5.3. Resolving screw dislocations in IF steels

An interstitial-free (IF) steel with 2 % silicon, deformed in tension to 1 % strain, was selected to illustrate the potential of ECCI for comprehensive dislocation characterisation through contrast analysis, analogous to that applied in TEM [10]. The analysis is synthesised in Fig. 8.

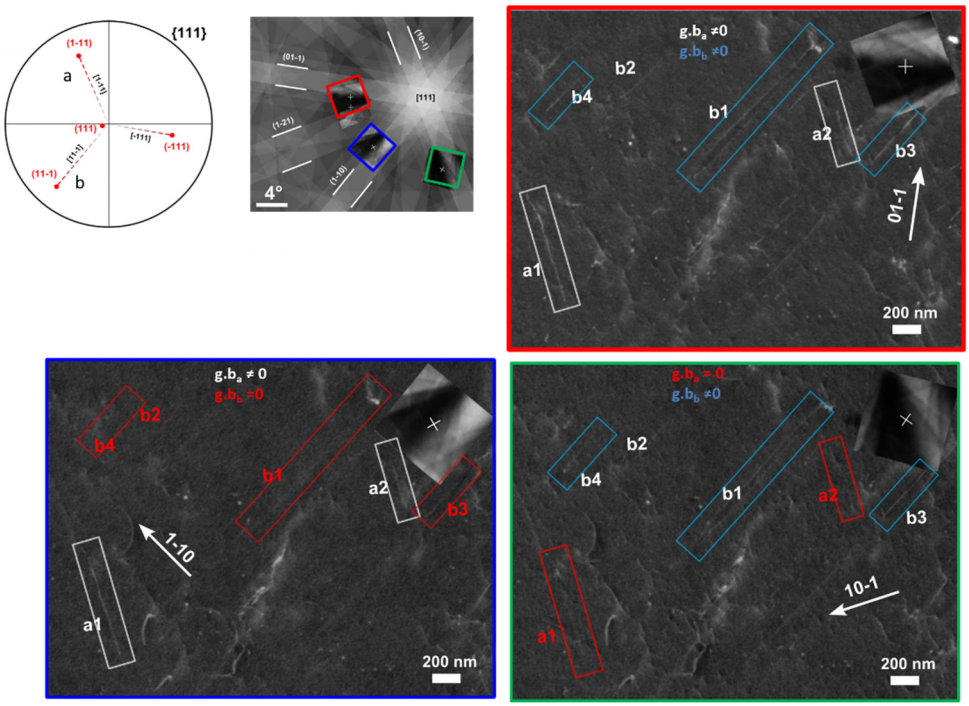

Figure 8. ECC images acquired under different channelling conditions. The diffraction vectors (**g**) are indicated by arrows: **g** = (01-1), **g** = (1-10), **g** = (10-1), **g** = (1-21) (not shown). Dislocations are labelled as a and b [13].

At low deformation levels, the dislocations in bcc IF-steel are expected to be primarily screw dislocations with Burgers vectors **b** = ½<111>. The conventional TEM **g**.**b** = 0 invisibility criterion (where **b** is the Burgers vector and **g** is the diffraction vector) can thus be applied.

A backscattered electron image was acquired from a surface-prepared specimen taken from the tensile sample. The orientation of the target grain was previously determined by EBSD. The grain of interest had an orientation near the [111] zone axis, as shown in the simulated EBSD pattern (at 0° tilt). In this orientation, the three other <111> dislocation lines are inclined at roughly 20° from the sample surface, with projections in the observation plane approximately 120° apart from one another. Their orientations are plotted on the stereographic projection in Fig. 8 (shown as fading dotted lines).

HR-SACPs were superimposed on the simulated pattern and used to set up four channelling conditions for the acquisition of the corresponding ECC images (three of which are shown in Fig. 8, boxed in red, green, and blue). The sample was tilted up to 15° and rotated to reach these four different **g** vectors.

Two sets of dislocations, with line directions labelled a and b (consistent with two of the nearly in-plane <111> line directions), are visible in the ECC images.

Imaging under the four different channelling conditions reveals contrast variations consistent with the dislocations being <111> screw dislocations. The dislocations labelled a1 and a2, with line directions [1-11], are visible with **g** = (01-1), **g** = (1-10), and **g** = (1-21) (all for which **g**.**b** ≠ 0) and invisible (highlighted in red in Fig. 8) with **g** = (10-1) (**g**.b = 0). Likewise, the dislocations labelled b1–b4, with line directions [11-1], are visible with **g** = (01-1), **g** = (10-1), and **g** =(1-21), but invisible (highlighted in red in Fig. 8) with **g** = (1-10).

This analysis demonstrates that by accurately setting up channelling conditions using HR-SACPs, robust contrast analysis can be carried out in fine polycrystalline materials.

6. CONCLUSION AND FUTURE CHALLENGES

ECCI has emerged as a powerful and accessible SEM-based technique for visualising and characterising crystallographic defects, such as dislocations, twins, and stacking faults, in bulk materials without the need for sample thinning. This tutorial has reviewed the fundamental principles of ECCI, as well as the practical methodologies for setting channelling conditions. Through advanced application examples, such as resolving dislocations in GaN, UO_2, and IF-steel, ECCI has demonstrated its capability to bridge the gap between TEM and SEM, offering high-resolution imaging of defects in a wide range of materials.

Despite its advantages, ECCI faces several challenges and limitations. ECCI is surface-sensitive, requiring high-quality surface preparation to avoid artefacts. High-precision orientation control ($\leq 0.1°$) is critical for ECCI but can be challenging to achieve in practice. Contrast analysis in ECCI can be enriched by a good understanding of electron diffraction theory.

Future advancements in detector technology, AI-assisted analysis, and in-situ experimentation are expected to further enhance ECCI capabilities for application in emerging materials. As ECCI continues to evolve, it promises to deepen our understanding of defect behaviour and microstructure-property relationships, making it an indispensable tool for materials characterisation in both research and industry.

7. REFERENCES

[1] Reimer L and Kohl H 2008 *Transmission electron microscopy. 5th edition*. [New York, NY: Springer]
[2] Coates D G 1967 *Phil. Mag.* **16** 1179-1184
[3] Booker G R, *et al.* 1667 *Phil. Mag.* **16** 1185-1191
[4] Ben Saada M 2017 *Étude du comportement visco-plastique du dioxyde d'uranium : quantification par analyse EBSD et ECCI des effets liés aux conditions de sollicitation et à la microstructure initiale*. PhD thesis. [Metz, France: Université de Lorraine]
[5] Mansour H, *et al.* 2019 *Ceramics Int.* **45** 18666-18671
[6] Trager-Cowan C, *et al.* 2020 *IOP Conf. Ser.: Mater. Sci. Eng.* **891** 012023
[7] Fan S, *et al.* 2022 *J. Appl. Phys.* **132** 105302
[8] Chen F, *et al.* 2025 *Acta Materialia* **301** 121622
[9] Gutierrez-Urrutia I, *et al.* 2009 *Scripta Materialia* **61** 737-740
[10] Mansour H, *et al.* 2014 *Scripta Materialia* **84-85** 11-14
[11] Guyon J, *et al.* 2015 *Ultramicroscopy* **149** 34-44
[12] Kerns R D, *et al.* 2020 *Ultramicroscopy* **210** 112915
[13] Mansour H 2016 *Caractérisation des défauts cristallins au MEB par canalisation d'électrons assistée par diagrammes pseudo-Kikuchi haute résolution: application à l'acier IF, UO_2 et TiAl*. PhD thesis. [Metz, France: Université de Lorraine]
[14] Rahmoune H, *et al.* 2026 *Advanced diffraction techniques in SEM for microstructural characterisation of semiconductors such as GaN*. in: Book of Tutorials and Abstracts of the EMAS 2026 Regional Workshop: Topical Conf. Electron Backscatter Diffraction (Gif-sur-Yvette, France; 14-17 June 2026)
[15] Reimer L. 1998 Scanning electron Microscopy. Physics of image formation and microanalysis. (2nd edition) [Berlin-Heidelberg, Germany: Springer-Verlag]
[16] Howie A and Whelan M J 1961 *Proc. R. Soc. Lond. A* **263** 217-237
[17] Hirsch P B and Humphreys C J 1970 *Theory of scanning electron microscope channeling patterns for normal and tilted specimens*. in: Proc. 7th Int. Congress Electron Microscopy (IFSEM). (Grenoble, Franec) **I** 229-230
[18] Spencer J P, *et al.* 1972 *Phil. Mag.* **26** 193-213

[19] Winkelmann A, *et al.* 2007 *Ultramicroscopy* **107** 414-421
[20] Wilkinson A J and Hirsch P B 1997 *Micron* **28** 279-308
[21] Zaefferer S and Elhami N 2014 *Acta Materialia* **75** 20-50
[22] Humphreys C J 1979 *Rep. Prog. Phys.* **42** 1825
[23] Williams D B and Carter C B 2001 *Transmission electron microscopy*. [Berlin-Heidelberg, Germany: Springer]
[24] Crimp M A, *et al.* 2001 *Philos. Mag. Lett.* **81** 833-837
[25] Maloufi N and Mansour H 2018 *L'imagerie par contraste de canalisation des électrons (ECCI)*. Chapter XVIII. in: Microscopie électronique à balayage et microanalyses (new edition). (Brisset F and Repoux M; Eds.) [Les Ulis, France: EDP Sciences] 633-652
[26] Maloufi N. 2021 *Imagerie par contraste de canalisation des électrons (ECCI) et défauts cristallins*. Techniques de l'Ingénieur M4145.
[27] Clarke D R and Howie A 1971 *Phil. Mag.* **24** 959-971 and 973-979
[28] El-Khairaoui N, *et al.* 2026a Electron diffraction and imaging in SEM: A flexible timepix3-based detector for both reflection and transmission. in: Book of Tutorials and Abstracts of the EMAS 2026 Regional Workshop: Topical Conf. Electron Backscatter Diffraction (Gif-sur-Yvette, France; 14-17 June 2026)
[29] El-Khairaoui N, *et al.* 2026b A single multi-configuration direct electron detector for various electron imaging and diffraction-based techniques in SEM 10.48550/arXiv.2605.18386
[30] Qaiser M H, *et al.* 2026 *J. Appl. Cryst.* **59** 530-551
[31] Beausir B and Fundenberger J J 2017 Analysis tools for electron and X-ray diffraction, ATEX - software, www.atex-software.eu. [Metz, France: Université de Lorraine]
[32] Lafond C, *et al.* 2018 *Ultramicroscopy* **186** 146-149
[33] Gallet J, *et al.* 2022 *Mater. Characterization* **194** 112358
[34] Ben Saada M, *et al.* 2017 *Mater. Characterization* **133** 112-121
[35] Ben Saada M, *et al.* 2021 *J. Nucl. Mater.* **545** 152632
[36] Nakamura S 1988 *Science* **281** 956-961
[37] Mishra U K, *et al.* 2002 *AlGaN/GaN HEMTs , an overview of device operation and applications*. in: Proc. IEEE **90** 1022-1031
[38] Pimputkar S, *et al.* 2009 *Nature Photon.* **3** 180-182
[39] Lester S D, *et al.* 1995 *Appl. Phys. Lett.* **66** 1249
[40] Speck J S and Rosner S J 1999 *Physica B* **273-274** 24-32
[41] Picard Y N, *et al.* 2009 *Scripta Materialia* **61** 773-776
[42] Naresh-Kumar, *et al.* 2012 *Phys. Rev. Lett.* **108** 135503